

# Estimating false inclusion rates in penalized regression models

Patrick Breheny  
 Department of Biostatistics  
 University of Iowa

June 6, 2022

---

## Abstract

Penalized regression methods are an attractive tool for feature selection with many appealing properties, although their widespread adoption has been hampered by the difficulty of applying inferential tools. In particular, the question "How reliable is the selection of those features?" has proved difficult to address, partially due to the complexity of defining a false discovery in the penalized regression setting. Here, I define a false inclusion as a variable that is independent of the outcome regardless of whether other variables are conditioned on. This definition permits straightforward estimation of the number of false inclusions. Theoretical analysis and simulation studies demonstrate that this approach is quite accurate when the correlation among predictors is mild, and slightly conservative when the correlation is moderate. Finally, the practical utility of the proposed method is illustrated using gene expression data from The Cancer Genome Atlas and GWAS data from the Myocardial Applied Genomics Network.

---

## 1 Introduction

Penalized regression is an attractive methodology for dealing with high-dimensional data where classical likelihood approaches to modeling break down. However, its widespread adoption has been hindered by a lack of inferential tools. In particular, penalized regression is very useful for variable selection, but the question "How reliable are those selections?" has proved difficult to address. As I will argue in this paper, this difficulty is partially due to the complexity of defining a "false discovery" in the penalized regression setting.

In this paper, I will focus mainly on the lasso for linear regression models (Tibshirani, 1996), although the idea is very general and can be extended to a variety of other regression models and penalty functions. In particular, suppose we use the lasso to select 10 variables from a pool of potentially important features. This paper addresses the question, "How many of those selections would likely have occurred by chance alone?"

There has been a fair amount of recent work on the idea of hypothesis testing in the high-dimensional penalized regression setting. A comprehensive review is beyond the scope of this paper, but it is worth introducing two approaches to which I will compare the method proposed in this paper. One approach is to split the sample into two parts, using the first part for variable selection and the second part for hypothesis testing. This idea was first introduced in Wasserman and Roeder (2009), who studied the problem using a single split of the data set. Meinshausen et al. (2009) extended this approach by considering multiple random splits and, in a sense, averaging the results. Dezeure et al. (2015) provides a comprehensive review of this approach and the details involved.

A different approach, proposed in Lockhart et al. (2014), is to test the significance of adding a variable along the solution path as we relax the degree of penalization, conditional on the other variables already included in the model. This approach is conceptually similar to the classical idea of an  $F$ -test, but with appropriate modifications made to adjust for the fact that we have searched over a large pool of potential predictors, rather than prespecifying

the feature to be added. This approach is also described, along with several other approaches to inference for the lasso, in Hastie et al. (2015).

In this paper, I introduce a weaker definition of false discovery than what is considered in Wasserman and Roeder (2009), Lockhart et al. (2014), or any other approach that I am aware of. I refer to this notion as a *false inclusion* to emphasize that what is being proposed is not an alternative method for controlling the same quantity, but rather an entirely different quantity to be controlled altogether. This idea is formally defined in Section 2 along with an estimator for the false inclusion rate. The remainder of the paper considers the accuracy of this estimator in a variety of settings, using both theoretical arguments and simulated and real data sets.

## 2 False inclusion rates

Consider the linear model with usual distributional assumptions:

$$\mathbf{y} = \mathbf{X}\boldsymbol{\beta} + \boldsymbol{\varepsilon}$$

$$\varepsilon_i \stackrel{\text{iid}}{\sim} N(0, \sigma^2),$$

where  $\mathbf{y}$  denotes the response and  $\mathbf{X}$  the  $n \times p$  design matrix, with  $n$  denoting the number of independent observations and  $p$  the number of features. Without loss of generality, we assume throughout that the responses and covariates are centered so that the intercept term can be ignored. We are interested in studying the lasso estimator  $\hat{\boldsymbol{\beta}}$ , defined as the quantity that minimizes

$$\frac{1}{2n} \|\mathbf{y} - \mathbf{X}\boldsymbol{\beta}\|^2 + \lambda \|\boldsymbol{\beta}\|_1,$$

where  $\|\boldsymbol{\beta}\|_1 = \sum_j |\beta_j|$ . Here, the usual least-squares loss is used to measure the fit of the model and the  $L_1$  norm is used to penalize large values of  $\boldsymbol{\beta}$ , with  $\lambda$  controlling the tradeoff between the two.

An appealing aspect of using the lasso to estimate  $\boldsymbol{\beta}$  is that the resulting estimates are sparse: some coefficients will be nonzero, but for many,  $\hat{\beta}_j = 0$ . In this paper, we say that a feature for which  $\hat{\beta}_j \neq 0$  is “included” in the model. Note that this will be a function of  $\lambda$ ; for a large enough value of  $\lambda$ ,  $\hat{\boldsymbol{\beta}} = \mathbf{0}$ , but as we lower  $\lambda$ , more variables will be included. To address the expected number of false inclusions in a lasso model, we begin by considering the orthonormal case, then turn our attention to the general case.

### 2.1 Orthonormal case

For a given value of the regularization parameter  $\lambda$ , let  $\mathbf{r} = \mathbf{y} - \mathbf{X}\hat{\boldsymbol{\beta}}$  denote the residuals. The Karush-Kuhn-Tucker (KKT) conditions are both necessary and sufficient for any solution  $\hat{\boldsymbol{\beta}}$ :

$$\begin{aligned} \frac{1}{n} \mathbf{x}'_j \mathbf{r} &= \lambda \text{sign}(\hat{\beta}_j) && \text{for all } \hat{\beta}_j \neq 0 \\ \frac{1}{n} |\mathbf{x}'_j \mathbf{r}| &\leq \lambda && \text{for all } \hat{\beta}_j = 0. \end{aligned}$$

Letting  $\mathbf{X}_{-j}$  and  $\boldsymbol{\beta}_{-j}$  denote the portions of the design matrix and coefficient vector that remain after removing the  $j$ th feature, let  $\mathbf{r}_j = \mathbf{y} - \mathbf{X}_{-j}\hat{\boldsymbol{\beta}}_{-j}$  denote the partial residuals with respect to feature  $j$ . The KKT conditions thus imply that

$$\begin{aligned} \frac{1}{n} |\mathbf{x}'_j \mathbf{r}_j| &> \lambda && \text{for all } \hat{\beta}_j \neq 0 \\ \frac{1}{n} |\mathbf{x}'_j \mathbf{r}_j| &\leq \lambda && \text{for all } \hat{\beta}_j = 0 \end{aligned} \tag{2.1}$$

and therefore the probability that variable  $j$  is selected is

$$\mathbb{P} \left( \frac{1}{n} |\mathbf{x}'_j \mathbf{r}_j| > \lambda \right).$$

This indicates that if we are able to characterize the distribution of  $\frac{1}{n}\mathbf{x}'_j\mathbf{r}_j$  under the null, we can estimate the number of false discoveries in the model. Indeed, this is straightforward in the case of orthonormal design ( $\frac{1}{n}\mathbf{X}'\mathbf{X} = \mathbf{I}$ ):

$$\frac{1}{n}\mathbf{x}'_j\mathbf{r}_j \sim N(\beta_j, \sigma^2/n). \quad (2.2)$$

Thus, if  $\beta_j = 0$ , we have

$$\mathbb{P}\left(\frac{1}{n}|\mathbf{x}'_j\mathbf{r}_j| > \lambda\right) = 2\Phi(-\lambda\sqrt{n}/\sigma).$$

These results are related to the expected number of false discoveries in the following theorem, the proof of which follows directly from the above by summing  $\mathbb{P}(\widehat{\beta}_j \neq 0)$  over all  $j \in \mathcal{N}$ .

**Theorem 1.** *Suppose  $\frac{1}{n}\mathbf{X}'\mathbf{X} = \mathbf{I}$ . Then for any value of  $\lambda$ ,*

$$\mathbb{E}|\mathcal{S} \cap \mathcal{N}| = 2|\mathcal{N}|\Phi(-\lambda\sqrt{n}/\sigma),$$

where  $\mathcal{S} = \{j : \widehat{\beta}_j \neq 0\}$  is the set of selected variables and  $\mathcal{N} = \{j : \beta_j = 0\}$  is the set of null variables.

To use this as an estimate, the unknown quantities  $|\mathcal{N}|$  and  $\sigma^2$  must be estimated. First,  $|\mathcal{N}|$  can be replaced by  $p$ , using the total number of variables as an upper bound for the null variables. The variance  $\sigma^2$  can be estimated by

$$\hat{\sigma}^2 = \frac{\mathbf{r}'\mathbf{r}}{n - |\mathcal{S}|}.$$

Dividing the residual sum of squares by the degrees of freedom of the lasso (Zou et al., 2007) is the simplest approach to estimating the residual variance, but other possibilities exist (e.g., Fan et al., 2012). This implies the following estimate for the expected number of false discoveries:

$$\widehat{\text{FD}} = 2p\Phi(-\sqrt{n}\lambda/\hat{\sigma}) \quad (2.3)$$

and, as an estimate of the false discovery rate:

$$\widehat{\text{FDR}} = \frac{\widehat{\text{FD}}}{|\mathcal{S}|}. \quad (2.4)$$

## 2.2 Definition in the general case

The case of correlated variables, however, is considerably more complex. Consider the causal diagram presented in Figure 1. In this situation, variable  $A$  could never be considered a false discovery: it has a direct causal relationship with the outcome  $Y$ . Likewise, if variable  $C$  were selected, this would obviously count as a false discovery –  $C$  has no relationship, direct or indirect, to the outcome.

Variable  $B$ , however, occupies a gray area as far as false discoveries are concerned.  $B$  and  $Y$  are not independent, but they are conditionally independent given  $A$ . From a modeling perspective,  $B$  may be quite useful in predicting  $Y$ , but only if  $A$  is not already in the model. For the sake of comparison, most work in the area, such as the sample splitting approaches of Wasserman and Roeder (2009) and Meinshausen et al. (2009), consider  $B$  a false discovery, as its associated regression coefficient would be zero in the full data generating process. However, the pathway based approach of Lockhart et al. (2014) would consider  $B$  a false discovery for some values of  $\lambda$  but not for others, depending on whether  $A$  has been included in the model yet or not.

The central argument of this paper is that estimating the number of false selections arising from variables like  $B$  is inherently complicated and requires complex approaches (either in the mathematical or computational

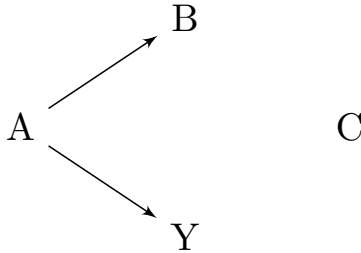


Figure 1: Causal diagram depicting three types of features and their relationship to the outcome.

sense); *however*, simple approaches like the one derived in Section 2.1 are still useful in terms of estimating false selections arising from variables like  $C$ .

Here, I define a *noise feature* to be a variable like  $C$ , that has no causal path (direct or indirect) between it and the outcome, and a *false inclusion* as the selection of a noise feature. Again, this is in contrast to most other work, which considers any variable with  $\beta_j = 0$  to be a false discovery, a definition that would include a variable like  $B$  in the diagram.

The proposed definition has several advantages. First, when two variables (like  $A$  and  $B$ ) are correlated, it is often difficult to distinguish between which of them is driving changes in  $Y$  and which is merely correlated with  $Y$ . As we will see, this causes any approach that defines false discoveries according to  $\beta_j = 0$  to be conservative, especially in high dimensions.

Second, in many scientific applications, discovering variables like  $B$  is not problematic. For example, two genetic variants in close proximity to each other on a chromosome will be highly correlated. Although it is obviously desirable to identify which of the two is the causal variant, locating a nearby variant is also an important scientific achievement, as it narrows the search to a small region of the genome for future follow-up studies.

The final advantage is clarity. Whether or not a variable is a false inclusion depends only on the relationships between variables, not whether those variables have been included in the model or not. In contrast, interpreting the results from the pathway-based test of Lockhart et al. (2014) can be challenging, as the definition of the null hypothesis is constantly changing with  $\lambda$ .

### 3 Independent noise features

#### 3.1 Theory

The conditions of Section 2.1 clearly do not hold in settings for which penalized regression is typically used. Thankfully, they can be relaxed in two important ways that make the results more widely applicable. First, the predictors do not have to be strictly orthogonal in order for the estimator to work; they can simply be uncorrelated. Second, this condition of being uncorrelated applies only to the noise features – i.e., the variables like  $C$  in Figure 1; variables like  $A$  and  $B$  can have any correlation structure.

To make these statements concrete, let  $\mathcal{A}, \mathcal{C}$  partition  $\{1, 2, \dots, p\}$  such that  $\beta_j = 0$  for all  $j \in \mathcal{C}$  and the following condition holds:

$$\lim_{n \rightarrow \infty} \frac{1}{n} \mathbf{X}' \mathbf{X} = \begin{bmatrix} \Sigma_{\mathcal{A}} & \mathbf{0} \\ \mathbf{0} & \Sigma_{\mathcal{C}} \end{bmatrix}.$$

Under this definition, the opening remarks of this section can be stated precisely in the following theorem.

**Theorem 2.** *Suppose  $\Sigma_{\mathcal{C}} = \mathbf{I}$ . Then for any  $j \in \mathcal{C}$  and for  $\lambda_n$  such that the sequence  $\sqrt{n}\lambda_n$  is bounded,*

$$\frac{1}{\sqrt{n}} \mathbf{x}'_j \mathbf{r}_j \xrightarrow{d} N(0, \sigma^2).$$

Theorem 2 shows that if the noise features are uncorrelated,  $\frac{1}{n} \mathbf{x}'_j \mathbf{r}_j$  behaves precisely as it did (cf. equation 2.2) in Section 2.1. Thus, estimators (2.3) and (2.4) will likely yield accurate approximations to estimating the

false inclusion rate in this setting (depending on the sample size, of course). The technical condition requiring  $\sqrt{n}\lambda_n$  to be bounded is only necessary so that the estimate  $\hat{\beta}$  will be  $\sqrt{n}$ -consistent; without it (i.e., for large values of  $\lambda$ ),  $\frac{1}{n}\mathbf{x}'_j\mathbf{r}_j$  will converge to a random variable with a variance larger than  $\sigma^2$  due to underfitting.

### 3.2 Simulation

To illustrate the consequences of Theorem 2, let us carry out the following simulation study, with both a “low-dimensional” ( $n > p$ ) and “high-dimensional” ( $n < p$ ) component. Motivated by Figure 1, three types of features will be included:

- Causative: Six variables with  $\beta_j = 1$
- Correlated: Each causative feature is correlated ( $\rho = 0.5$ ) with  $m$  other features;  $m = 2$  for the low-dimensional case and 9 for the high-dimensional case
- Noise: Independent noise features are added to bring the total number of variables up to 60 in the low-dimensional case and 600 in the high-dimensional case

The causative, correlated, and noise features correspond to variables A, B, and C, respectively, in Figure 1. In each setting, the sample size was  $n = 100$ , while the total number of causative/correlated/noise features was 6/12/42 for the low-dimensional setting and 6/54/540 for the high-dimensional setting. The results of the simulation are shown in Figure 2.

As Theorem 2 implies, estimators (2.3) and (2.4) are quite accurate, on average, when the noise features are independent. The estimated number of false inclusions and false inclusion rate (FIR) are both somewhat conservative, as we would expect from using  $p$  as an upper bound for the number of noise features (e.g., in the high-dimensional case,  $p = 600$  but  $|\mathcal{C}| = 540$ ). However, the effect is slight in this setting. For example, in the high-dimensional case at  $\lambda = 0.55$ , the actual false inclusion rate was 5%, while the estimated rate was 6.5%.

Being able to estimate false inclusion rates means we can use them to select the regularization parameter  $\lambda$ . For example, we could choose  $\lambda$  to be the smallest value of  $\lambda$  such that  $\widehat{\text{FIR}}(\lambda) < 0.1$ . Figure 3 compares this approach (“LassoFIR”) with several other methods for selecting  $\lambda$  in terms of the number of each type of feature the method selects on average. For LassoFIR, univariate testing (i.e., marginal regression), and sample splitting (using the `hdi` package, Dezeure et al., 2015), the nominal false discovery rates were set to 10%. For cross-validation, the value of  $\lambda$  minimizing the cross-validation error was selected. Finally, for the covariance test approach (using the `covTest` package, Lockhart et al., 2014), which tests progression along a decreasing sequence of  $\lambda$  values, I selected the model  $\hat{\beta}(\lambda_k)$ , where  $k$  is the largest value for which the test for proceeding from  $\lambda_{k-1}$  to  $\lambda_k$  is significant at the  $p = 0.05$  level.

It is worth noting that both LassoFIR and univariate testing limit the fraction of selections due to noise features (to 5% and 7%, respectively, in the  $p = 60$  simulation) to the nominal rate, but claim nothing about the fraction arising from correlated features. This is obvious from the figure for univariate testing; for LassoFIR, the fraction of selected features coming from either the Correlated or Noise groups (i.e., all features with  $\beta_j = 0$ ) was 17% in the low-dimensional setting and 23% in the high-dimensional setting. Nevertheless, compared to univariate testing, the LassoFIR approach has two distinct advantages. Figure 3 shows that using a penalized regression approach both diminishes the number of merely correlated features selected and improves power to detect the truly causative features.

Among the penalized regression approaches, cross-validation is a considerable outlier, with no protection against the selection of large numbers of noise features. In the high-dimensional case, cross-validation selected over 30 noise features on average, and is omitted from the plot so as not to obscure the performance of the other methods.

The sample splitting and covariance test approaches, on the other hand, greatly limit the number of both noise features and correlated features selected by the lasso model. By considering all features with  $\beta_j = 0$  to be false discoveries, the sample splitting approach behaves quite conservatively, and has considerably less power to detect the causative features than any of the other methods considered. As one might expect, the covariance test approach, which adopts a perspective in between that of sample splitting and false inclusion rates with respect

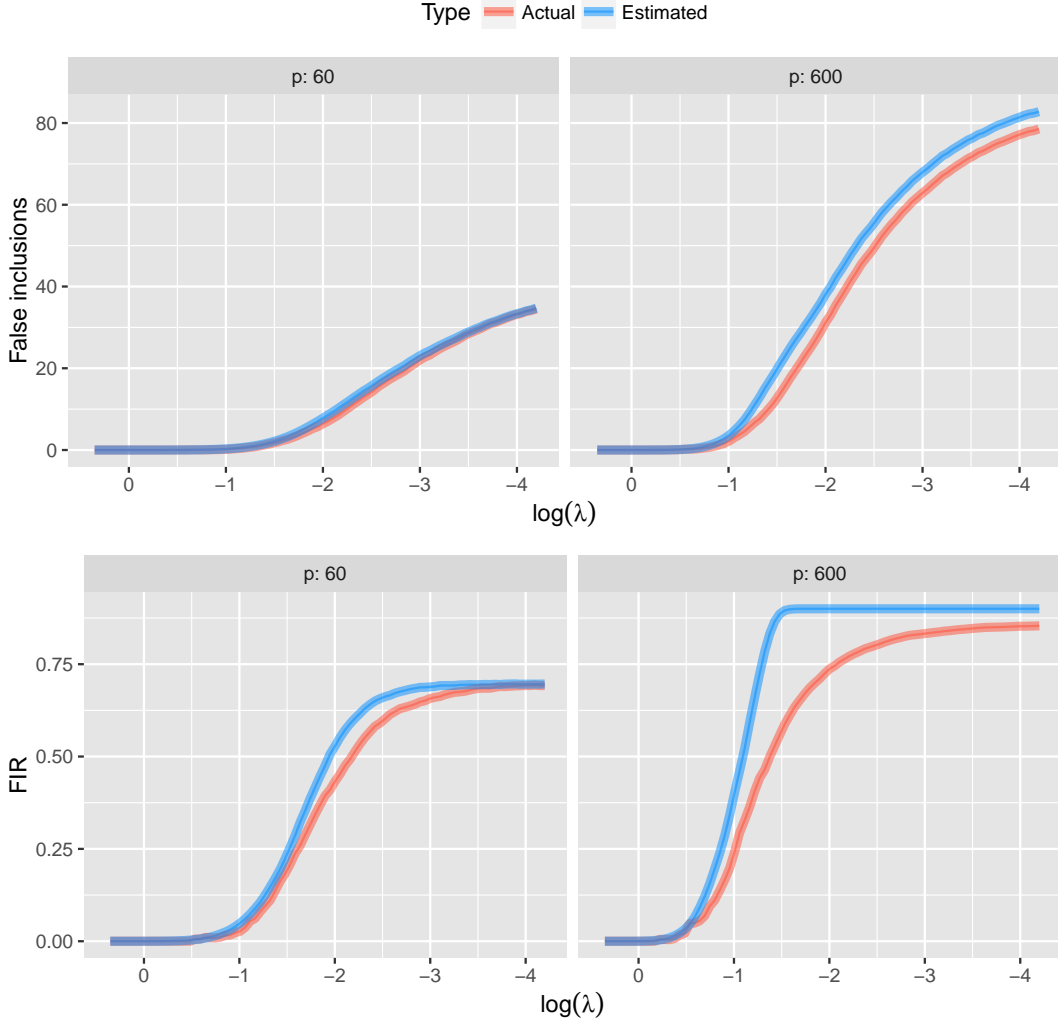


Figure 2: Accuracy of estimators (2.3) and (2.4) in the case of independent noise features.

to false discoveries, has intermediate power to detect causative features, finding more than sample splitting but fewer than FIR.

## 4 Correlated noise features

### 4.1 Theory

The simulation results of Section 3.2 are something of a best case scenario for the proposed method, since the variables in  $\mathcal{C}$  were independent and we know by Theorem 2 that the estimator is valid in this case. When noise features are correlated, we will see that the estimator becomes conservative.

Unfortunately, the case of correlated noise features is significantly less mathematically tractable, making it harder to construct rigorous proofs about the performance of the proposed method in this case. Nevertheless, I offer the following conjecture about the conservative nature of the estimates when noise features are correlated. A proof for the  $p = 2$  case is given in the Appendix; the proof is somewhat interesting on its own, offering some insight into why the estimates are conservative and how a proof for arbitrary  $p$  might be constructed.

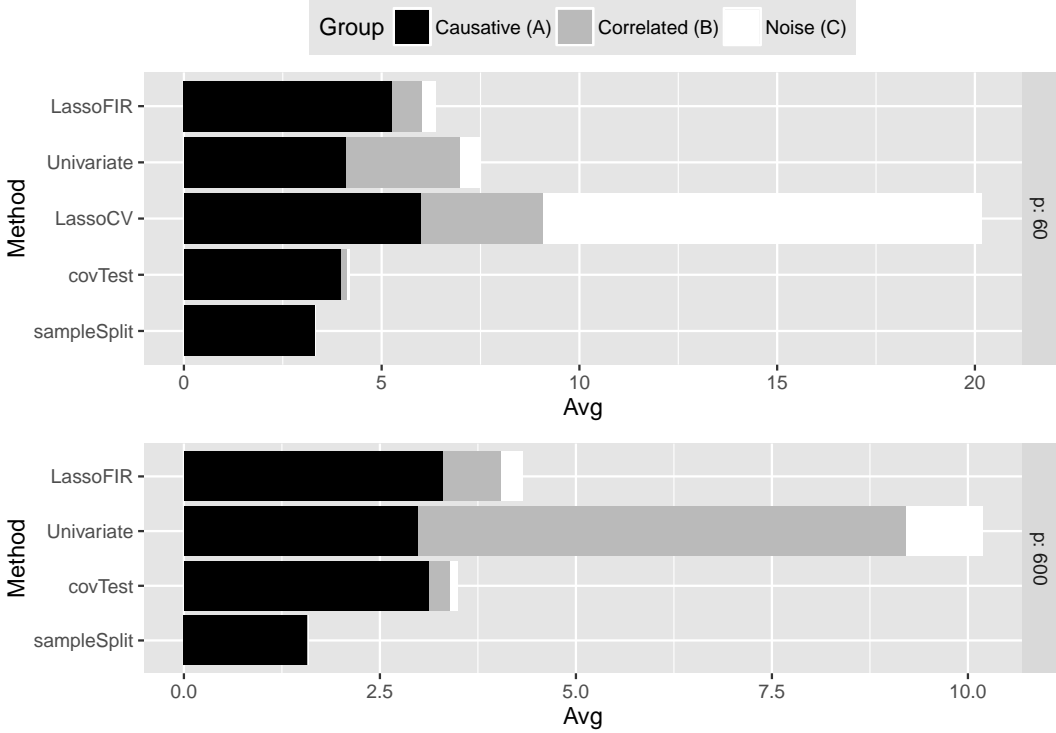


Figure 3: Average number of each type of feature selected by various methods for the simulation setup in Section 3.2. Cross-validation is omitted from the high-dimensional ( $p = 600$ ) plot due to the very large number of noise features it selects, which dominates the plot when included.

**Conjecture.** *Using the notation of Section 3.1, for any  $\lambda$  and  $\Sigma_C$ , we have*

$$\mathbb{E} |\mathcal{S} \cap \mathcal{N}| \leq 2 |\mathcal{N}| \Phi(-\lambda \sqrt{n}/\sigma).$$

The basic intuition behind this conjecture is that if two noise features are correlated, the lasso (and many other penalized regression methods) will tend to select a single feature rather than both. Thus, the uncorrelated case is not just mathematically convenient, it also represents a worst case scenario with respect to the number of noise features that we can expect to be falsely selected. We examine the consequences of this conservatism in the next section.

## 4.2 Simulation

To investigate the robustness of the proposed FIR estimator in the presence of moderate correlation, let us carry out the following simulation. The generating model contains 6 independent causative features and 494 correlated noise features, with a 1:1 signal-to-noise ratio ( $n = 100$ ,  $p = 500$ ,  $R^2 = 0.5$ ). The noise features are given an autoregressive correlation structure with  $\text{Cor}(\mathbf{x}_j, \mathbf{x}_k) = 0.8^{|j-k|}$ . The results of the simulation are shown in Figure 4.

Compared to Figure 2, the FIR estimates are somewhat more conservative in this case, although still quite accurate – certainly accurate enough to be useful in practice. For example, at  $\lambda = 0.43$ , the true false inclusion rate was 14%, while the estimated rate according to (2.3) was 20%.

This simulation illustrates that although its derivation is based on independent noise features, the proposed FIR estimator is reasonably robust to the presence of correlation. Furthermore, to the extent that it is inaccurate, it provides a conservative estimate of the false inclusion rate, suggesting (as the conjecture indicates) that the approach provides some measure of control over the false inclusion rate, at least on average.

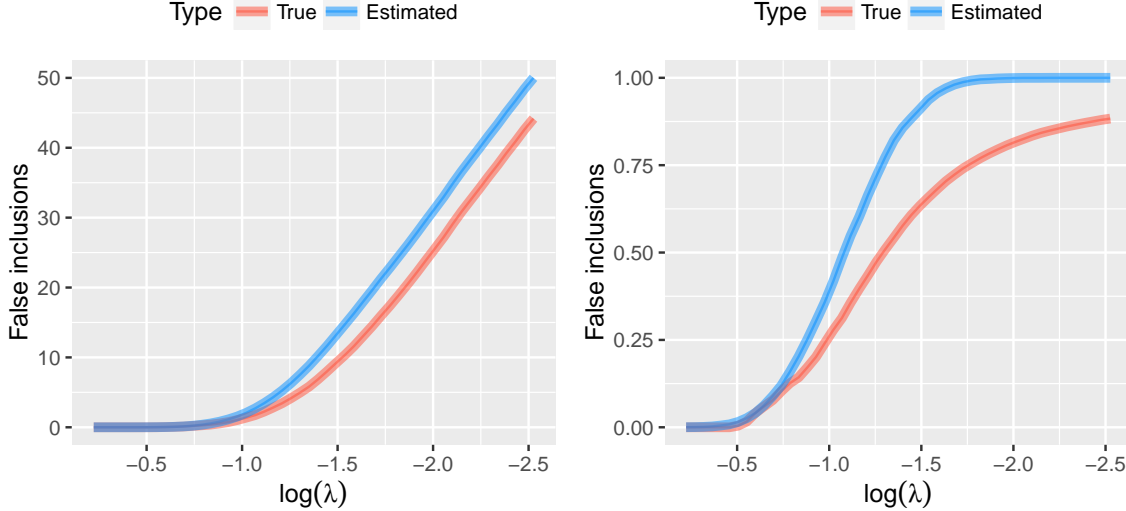


Figure 4: Accuracy of estimators (2.3) and (2.4) in the case of (autoregressive) correlated noise features.

## 5 Permutation approach

As correlation between noise features becomes more extreme, estimate (2.3) becomes increasingly conservative. To take an extreme example, suppose that the correlation structure from Section 4.2 was exchangeable instead of autoregressive:  $\text{Cor}(\mathbf{x}_j, \mathbf{x}_k) = 0.8$  for all  $j, k$ . The results of this modification to the simulation (all other aspects remaining the same) are shown in Figure 5.

As one might expect, the estimates are far more conservative in this case. For example, at  $\lambda = 0.43$ , the estimated FIR is 23% even though the true FIR is only 1%. This is a consequence of the independence approximation, where (2.4) operates under the simplifying assumption that the selection of one noise feature does not affect the probability of other noise features being selected. Although usually reasonably accurate, that approximation is highly inaccurate here, where every noise feature is highly correlated with every other noise feature. As a result, the lasso tends to select only a single noise feature from this highly correlated set, while the independence-based estimate (2.3) indicates that it has likely selected, say, 7 or 8.

This phenomenon is not unique to penalized regression; substantial correlation among features causes problems with conventional false discovery rates as well (Efron, 2007). One widely used approach for controlling error rates while preserving correlation structures is to use a permutation approach (Westfall and Young, 1993), and a similar strategy may be applied in order to calculate false inclusion rates for penalized regression as well. The primary advantage of this approach is that it eliminates the conservatism of the analytic approach developed in Section 2, while the primary disadvantage is a greatly increased computational burden. In this section, I describe two permutation-based methods and apply them to the simulation shown in Figure 5.

### 5.1 Permuting the outcome

The simplest approach is simply to randomly permute the outcome  $\mathbf{y}$ , creating new outcomes  $\tilde{\mathbf{y}}^{(b)}$  for  $b = 1, 2, \dots, B$ . Then, for each permutation  $b$ , solve for the lasso path  $\tilde{\beta}^{(b)}(\lambda; \mathbf{X}, \tilde{\mathbf{y}}^{(b)})$ , estimate the average number of false inclusions for a given value of  $\lambda$

$$\widehat{\text{FI}}(\lambda) = \frac{\sum_b \#\{\tilde{\beta}_j^{(b)}(\lambda) \neq 0\}}{B},$$

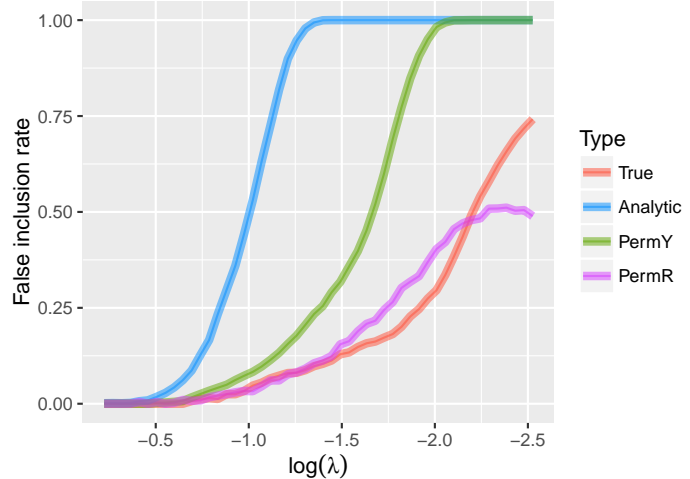


Figure 5: Accuracy of the analytic (2.4), permute-the-outcome (“PermY”, (5.1)), and permute-the-residuals (“PermR”) estimators in the case of (exchangeable) correlated noise features.

and the false inclusion rate using

$$\widehat{\text{FIR}}_Y(\lambda) = \frac{\widehat{\text{FI}}(\lambda)}{S(\lambda)}, \quad (5.1)$$

where  $S(\lambda)$  is the number of variables selected by the lasso using the original (i.e., not permuted) data.

This method is applied to the case of heavy exchangeable correlation in Figure 5. The method is considerably less conservative than the analytic approach, although still conservative for reasons that will be discussed in Section 5.2. For example, at  $\lambda = 0.43$ , the average estimated FIR is 4%, where the true value was 1% and the analytic approach yielded 23%.

By permuting  $Y$ , this approach constructs realizations of the data in which all features belong to  $\mathcal{C}$ , the set of noise features. Like (2.4), it limits the number of noise features selected but cannot be used to control the number of false discoveries in the sense of limiting selections from all variables with  $\beta_j = 0$ . In the hypothesis testing literature, this is referred to as “weak control” over the error rate.

## 5.2 Permuting the residuals

As seen in Figure 5, permuting the outcomes is still conservative in its estimation of FIR. The primary reason for this is that, provided that at least some features are *not* noise, the variance of  $Y$  can be separated into signal and noise; ideally we would permute only the noise, but by permuting the outcome we permute the signal as well. This has the effect, in a sense, of overestimating the noise present in the model; this is essentially the same phenomenon that occurs in Theorem 2 if the sequence  $\sqrt{n}\lambda_n$  is not bounded.

One alternative is, rather than permuting the outcome, to permute the residuals,  $\mathbf{r}(\lambda) = \mathbf{y} - \mathbf{X}\widehat{\boldsymbol{\beta}}(\lambda)$ , of the original lasso fit. The method is otherwise identical to that described in Section 5.1, with the notable exception that the residuals, unlike the outcomes, depend on  $\lambda$  and thus,  $B$  separate lasso solutions  $\widetilde{\boldsymbol{\beta}}^{(b)}(\lambda; \mathbf{X}, \mathbf{r}^{(b)})$  must be calculated at each value of  $\lambda$  (in Section 5.1, the same solutions could be used for all values of  $\lambda$ ), substantially increasing the computational burden.

Nevertheless, this increased computational cost does offer a benefit, as seen in Figure 5. Unlike the analytic and permute-the-outcome approaches, permuting the residuals is not conservative (it may, in fact, be somewhat liberal for small  $\lambda$  values as the model approaches saturation). For example, at  $\lambda = 0.29$ , the average estimated FIR is 8%, as was the true FIR, whereas the permute-the-outcome and analytic methods estimated FIRs of 16% and 90%, respectively.

The purpose of this manuscript is primarily to investigate the analytic approach to calculating false inclusion rates outlined in Section 2, with relatively less emphasis on the permutation approaches. In the opinion of the author, the analytic approach is almost always useful, since it can be calculated instantly. Whether one wishes to take the time to carry out the permutation approach, however, depends on context: how correlated the features are, how problematic a somewhat conservative estimate of FIR is, and how far along in the analytic process one is (initial exploration or final publication results). For a more detailed comparison of the analytic and permutation approaches in the context of genetic association studies, see Yi et al. (2015).

## 6 Case studies

### 6.1 Breast cancer gene expression study

As a case study in applying the proposed method to real data, we will analyze data on gene expression in breast cancer patients from The Cancer Genome Atlas (TCGA) project, available at <http://cancergenome.nih.gov/>. In this dataset, expression measurements of 17,814 genes, including BRCA1, from 536 patients are recorded on the log scale.

BRCA1 is a well-studied tumor suppressor gene with a strong relationship to breast cancer risk. Because BRCA1 is likely to interact with many other genes, including tumor suppressors and regulators of the cell division cycle, it is of interest to find genes with expression levels related to that of BRCA1. These genes may be functionally related to BRCA1 and are useful candidates for further studies.

For this analysis, I excluded 491 genes with missing data, resulting in a design matrix with  $p = 17,322$  predictors. The resulting FIR estimates for the lasso solution path are presented in Figure 6. Here, the FIR estimates indicate that many genes are predictive of BRCA1 expression – we can safely select 55 variables before the false inclusion rate exceeds 10%. This make sense scientifically, as a large number of genes are known to affect BRCA1 expression through a variety of mechanisms, and the sample size here is sufficient that we should be able to identify many of them.

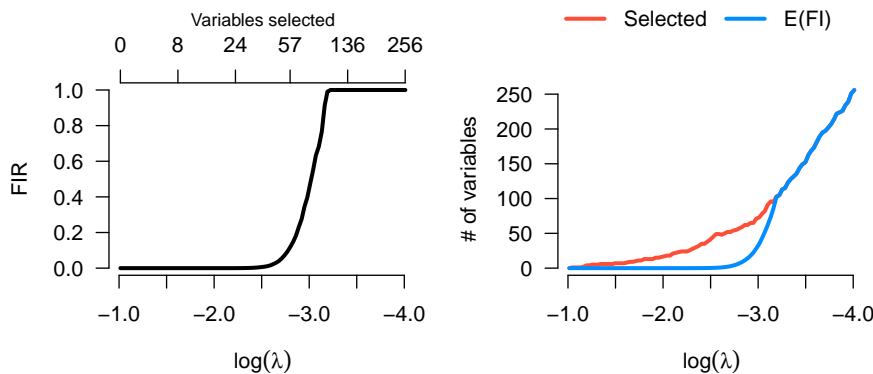


Figure 6: False inclusion rate estimates for a lasso model applied to the breast cancer TCGA data.

In contrast, the `covTest` procedure selects somewhere between 2 and 6 features (depending on the stopping rule one applies to the sequence of  $p$ -values), while sample splitting selects just a single feature. Although the FIR estimates are slightly conservative as discussed in Section 4, this matters far less in practice than the definition of a false discovery in the first place. This example clearly illustrates how conservative the definition  $\beta_j = 0$  is in practice, especially with high-dimensional data.

It is also worth comparing these results to the selection of  $\lambda$  by cross-validation (CV). For the TCGA data,  $\lambda = 0.0436$  minimizes the CV error. The estimated FIR at this value, however, is 77%, indicating that although this value of  $\lambda$  may be attractive from a prediction perspective, we cannot be confident that the variables selected by the model are truly related to the outcome. Indeed, it has long been recognized from a theoretical perspective that while the lasso has attractive variable selection and prediction properties, it cannot achieve both those aims simultaneously (Fan and Li, 2001). The FIR estimates illustrate this concretely:  $\lambda = 0.0436$  produces accurate

predictions, but a larger value,  $\lambda = 0.0627$ , is required in order to have confidence that noise features have been eliminated from the set of selected variables such that they comprise less than 10% of the total.

## 6.2 Minimax concave penalty

The FIR estimator follows directly from the KKT conditions for a given penalty, and it is straightforward to extend to other penalties. In fact, the KKT conditions for many penalties lead to the same expression (2.1) and therefore the same FIR estimator.

One such penalty is the minimax concave penalty, or MCP (Zhang, 2010). Briefly, the MCP produces sparse estimates like the lasso, but modifies the penalty such that the selected variables are estimated with less shrinkage towards zero (see the original paper for details). The main consequence of this is that MCP solutions tend to be more sparse than those of the lasso, in that they allow features to have larger regression coefficients, requiring fewer features to achieve the same predictive ability. To put it differently, for the lasso to estimate large coefficients accurately, it must lower  $\lambda$ , thereby increasing the number of noise features in the model and increasing the FIR. MCP, on the other hand, can estimate large coefficients accurately while still screening out the noise features, at least asymptotically (this is known as the “oracle property”).

To see how this works in practice, we can fit an MCP model to the TCGA data and compare its results to those of the lasso. For the value of  $\lambda$  minimizing CV error, both methods had similar predictive accuracy (cross-validated  $R^2 = 0.61$  for the lasso and 0.58 for MCP), but the MCP model used far fewer features (38 compared to 96 for the lasso). Consequently, for these values of  $\lambda$  the estimated FIR for MCP was much lower than that of the lasso: 5% compared to the lasso’s 77%. If we restrict the lasso FIR to 5% by increasing  $\lambda$ , its predictive accuracy falls to  $R^2 = 0.57$ .

This is representative of the relationship between lasso and MCP: the lasso can typically achieve slightly better prediction accuracy, but in doing so selects a large number of noise features. This pattern has been observed in simulation studies (e.g., Breheny and Huang, 2011), but FIR estimates offer a way to observe and assess this tradeoff in the analysis of real data.

This example also illustrates the ease with which the proposed estimator can be extended to other penalties. In addition to MCP, the SCAD (Fan and Li, 2001) and elastic net (Zou and Hastie, 2005) also have similar KKT conditions leading to (2.1) and thus requiring only trivial modifications to the FIR estimator.

## 6.3 Genetic association study of cardiac fibrosis

As an additional example, let us also look at a genetic association study of cardiac fibrosis. The data come from the Myocardial Applied Genomics Network (MAGNet), which collected tissue and gene expression data on 313 human hearts along with genetic data using the Affymetrix Genome-Wide Human SNP Array 6.0. We are interested in the ratio of cardiomyocytes to fibroblasts in the heart tissue. An abundance of fibroblasts is indicative of cardiac fibrosis, which leads to heart failure. In this analysis, the goal is to discover single nucleotide polymorphisms (SNPs) associated with increased fibrosis. Here, we use the log of the cardiomyocyte:fibroblast ratio as the response, and SNPs with  $< 10\%$  missing data as the predictors, resulting in  $p = 660,496$  features. `mimimac2` was used to impute the missing genotypes that remained (Fuchsberger et al., 2015).

In contrast to the TCGA data, no features can be selected with any degree of confidence in the MAGNet data. For all values of  $\lambda$  in which features are selected, the FIR estimate is 100%. This is consistent with a traditional genome-wide association analysis, which also fails to identify any SNPs that are significant following a Bonferroni correction for multiple testing.

This negative example illustrates the usefulness of FIR estimates in terms of guarding against false positives. The efficiency with which methods like the lasso extend to high dimensions make analyses like this (with  $n = 313$  and  $p = 660,496$ ) feasible from a computational standpoint. However, there are important statistical considerations here that need to be accounted for; namely, with  $p$  so large, the probability of selecting noise features is so great that one cannot place any trust in the variables that the lasso selects. These considerations are clearly illustrated by the estimation of FIR, but are lost if one simply uses the lasso to identify the top  $|\mathcal{S}|$  SNPs (as in, e.g., Wu et al., 2009).

## 7 Discussion

The false inclusion rate estimator presented in this article is a straightforward, useful way of quantifying the reliability of feature selection for penalized regression models such as the lasso. Compared with other proposals such as the pathwise covariance test and sample splitting, FIR does not attempt to limit the selection of all variables with  $\beta_j = 0$ , only those which are truly noise in the sense of being independent of the outcome. Certainly, there is a place for those proposals, but the relaxed definition of a false discovery that we have pursued here has several advantages in practice, particularly in high dimensions. These advantages include greater power to detect features, no added computation cost, and a simple rate with a straightforward interpretation. Although the estimate can be conservative for highly correlated features, in most realistic settings this conservatism is mild.

The proposed estimator is easy to implement and is available (along with the permutation methods of Section 5) in the **R** package **ncvreg** (Breheny and Huang, 2011), which was used to fit all of the models presented in this paper (except where the **hdi** and **covTest** packages were used). The following bit of code demonstrates its use:

```
fit <- ncvreg(X, y, penalty="lasso")
obj <- fir(fit)
plot(obj)
```

This will fit a lasso model, estimate the FIR at each value of  $\lambda$  and assign it to an object, then plot the results, as in Figure 6.

The simplicity of the method makes it available at no added computational cost and very easy to generalize to new methods: the **fir** function in **ncvreg** also works for elastic net, SCAD, MCP, and Mnet (Huang et al., 2016) penalties. As with any statistic, there are limitations and one needs to be careful with interpretation, but FIR is a convenient model summary measure that is helpful in the selection of  $\lambda$  for penalized regression models as well as a useful estimate for the reliability of feature selection in such models.

## Acknowledgments

I would like to thank Jian Huang for fruitful discussions of this idea when it was still in its early stages, Ina Hoeschele for discussions of the permutation approach, and Ryan Boudreau for the MAGNet data of Section 6.3.

## Appendix

*Proof of Theorem 2.* Starting with the observation that  $\mathbf{r}_j = \mathbf{X}\boldsymbol{\beta} + \boldsymbol{\varepsilon} - \mathbf{X}_{-j}\hat{\boldsymbol{\beta}}_{-j}$ , for any  $j \in \mathcal{C}$  we have

$$\frac{1}{\sqrt{n}}\mathbf{x}'_j\mathbf{r}_j = \frac{1}{\sqrt{n}}\mathbf{x}'_j\boldsymbol{\varepsilon} + \left(\frac{1}{n}\mathbf{x}'_j\mathbf{X}_{-j}\right)\{\sqrt{n}(\boldsymbol{\beta}_{-j} - \hat{\boldsymbol{\beta}}_{-j})\}$$

The first term,  $\frac{1}{\sqrt{n}}\mathbf{x}'_j\boldsymbol{\varepsilon}$ , converges in distribution to  $N(0, \sigma^2)$  by the independence of  $\mathbf{x}_j$  and  $\boldsymbol{\varepsilon}$ . The second term,  $\frac{1}{n}\mathbf{x}'_j\mathbf{X}_{-j}$ , converges to zero by the assumption that  $\Sigma_{\mathcal{C}} = \mathbf{I}$  ( $\mathbf{x}_j$  is also independent of variables in  $\mathcal{A}$  since  $j \in \mathcal{C}$ ). Finally, the third term is bounded in probability provided that  $\sqrt{n}\lambda_n$  is bounded (Fan and Li, 2001). Therefore, by Slutsky's Theorem, the entire quantity converges in distribution to  $N(0, \sigma^2)$ .  $\square$

*Proof of Conjecture for the  $p = 2$  case.* Although investigation of the conjecture is complicated in higher dimensions, it can be shown in the  $p = 2$  case, and its proof lends some insight into why it may hold in higher dimensions. Let  $z_j = \frac{1}{n}\mathbf{x}'_j\mathbf{y}$ . We begin by noting that  $\mathbf{z}$  follows a multivariate normal distribution with mean  $\mathbf{0}$  and

$$\text{Var}(\mathbf{z}) = \frac{\sigma^2}{n} \begin{bmatrix} 1 & \rho \\ \rho & 1 \end{bmatrix},$$

where  $\rho$  denotes the correlation between  $\mathbf{x}_1$  and  $\mathbf{x}_2$ , and

$$2|\mathcal{N}|\Phi(-\lambda\sqrt{n}/\sigma) = \mathbb{P}(|z_1| > \lambda) + \mathbb{P}(|z_2| > \lambda). \quad (7.1)$$

A visual representation of this quantity is given in Figure 7. The shading represents whether 0 (white), 1 (light gray), or 2 (dark gray) features will be selected under this orthogonal approximation; the quantity in (7.1) can be found by integrating these constant regions with respect to the joint density of  $\mathbf{z}$ .

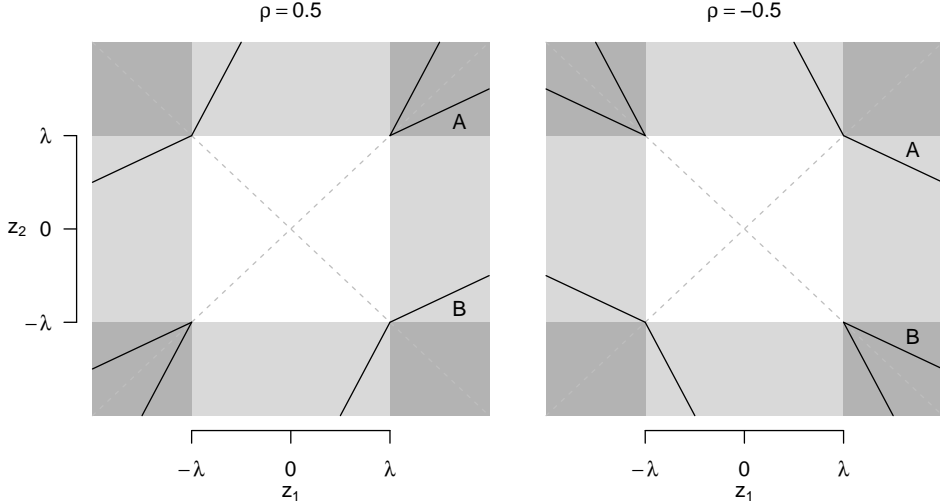


Figure 7: Illustration of how correlation affects selection in the bivariate case. Features  $\mathbf{x}_1$  and  $\mathbf{x}_2$  are positively correlated ( $\rho = 0.5$ ) on the left and negatively correlated ( $\rho = -0.5$ ) on the right.

In the case where  $\mathbf{x}_1$  and  $\mathbf{x}_2$  are non-orthogonal, the white region (where no features are selected) remains the same, but the conditions under which both features are selected (the light and dark gray regions) change. By working through the KKT conditions for the bivariate case under various conditions, we can determine these selection boundaries. For example, the boundary for  $\hat{\beta}_2 > 0$  given that  $\hat{\beta}_1 > 0$  (i.e., given that  $z_1 > \lambda$ ) is

$$\begin{aligned} \frac{1}{n} |\mathbf{x}_2' \mathbf{r}_2| > \lambda &\implies z_2 - \rho \hat{\beta}_1 > \lambda \\ &\implies z_2 > \rho z_1 + \lambda(1 - \rho). \end{aligned}$$

These boundaries are drawn in black on Figure 7; the preceding equation is the line just above the letter "A". As the figure illustrates, when  $\rho > 0$  the region over which  $\beta_1, \beta_2 \neq 0$  narrows in the upper right and lower left quadrants, and widens in the other two quadrants. Considering the difference  $\mathbb{E}|\mathcal{S} \cap \mathcal{N}| - \{\mathbb{P}(|z_1| > \lambda) + \mathbb{P}(|z_2| > \lambda)\}$ , we see that in many regions, the terms cancel out by integrating the same quantity over the same distribution. The differences lie in four pairs of triangular regions; one such pair is labeled "A" and "B" in the figure. The region A is where two variables are selected under orthogonality, but only one in the correlated case, while region B is where one variable is selected under orthogonality, but two are selected in the correlated case. However, because  $z_1$  and  $z_2$  are positively correlated in this scenario, the density at each point in A is higher than its corresponding point in B, and therefore

$$\mathbb{E}|\mathcal{S} \cap \mathcal{N}| < \mathbb{P}(|z_1| > \lambda) + \mathbb{P}(|z_2| > \lambda)$$

as the conjecture claims. The opposite scenario happens for  $\rho < 0$ , where region B now has the higher probability density, which again leads to a larger integral under orthogonality, with equality between the two quantities occurring only at  $\rho = 0$ .  $\square$

## References

BREHENY, P. and HUANG, J. (2011). Coordinate descent algorithms for nonconvex penalized regression, with applications to biological feature selection. *Annals of Applied Statistics*, **5** 232–253.

DEZEURE, R., BÜHLMANN, P., MEIER, L. and MEINSHAUSEN, N. (2015). High-dimensional inference: Confidence intervals,  $p$ -values and R-software **hdi**. *Statist. Sci.*, **30** 533–558.

EFRON, B. (2007). Correlation and large-scale simultaneous significance testing. *Journal of the American Statistical Association*, **102** 93–103.

FAN, J., GUO, S. and HAO, N. (2012). Variance estimation using refitted cross-validation in ultrahigh dimensional regression. *Journal of the Royal Statistical Society Series B*, **74** 37–65.

FAN, J. and LI, R. (2001). Variable selection via nonconcave penalized likelihood and its oracle properties. *Journal of the American Statistical Association*, **96** 1348–1360.

FUCHSBERGER, C., ABECASIS, G. R. and HINDS, D. A. (2015). minimac2: faster genotype imputation. *Bioinformatics*, **31** 782–784.

HASTIE, T., TIBSHIRANI, R. and WAINWRIGHT, M. (2015). *Statistical learning with sparsity: the lasso and generalizations*. CRC Press.

HUANG, J., BREHENY, P., LEE, S., MA, S. and ZHANG, C.-H. (2016). The Mnet method for variable selection. *Statistica Sinica*, **26** 903–923.

LOCKHART, R., TAYLOR, J., TIBSHIRANI, R. J. and TIBSHIRANI, R. (2014). A significance test for the lasso. *The Annals of Statistics*, **42** 413–468.

MEINSHAUSEN, N., MEIER, L. and BÜHLMANN, P. (2009). p-values for high-dimensional regression. *Journal of the American Statistical Association*, **104** 1671–1681.

TIBSHIRANI, R. (1996). Regression shrinkage and selection via the lasso. *Journal of the Royal Statistical Society Series B*, **58** 267–288.

WASSERMAN, L. and ROEDER, K. (2009). High dimensional variable selection. *Annals of Statistics*, **37** 2178.

WESTFALL, P. H. and YOUNG, S. S. (1993). *Resampling-based multiple testing: Examples and methods for p-value adjustment*. Wiley, New York.

WU, T., CHEN, Y., HASTIE, T., SOBEL, E. and LANGE, K. (2009). Genome-wide association analysis by lasso penalized logistic regression. *Bioinformatics*, **25** 714–721.

YI, H., BREHENY, P., IMAM, N., LIU, Y. and HOESCHELE, I. (2015). Penalized multimarker vs. single-marker regression methods for genome-wide association studies of quantitative traits. *Genetics*, **199** 205–222.

ZHANG, C. (2010). Nearly unbiased variable selection under minimax concave penalty. *Annals of Statistics*, **38** 894–942.

ZOU, H. and HASTIE, T. (2005). Regularization and variable selection via the elastic net. *Journal of the Royal Statistical Society Series B*, **67** 301–320.

ZOU, H., HASTIE, T. and TIBSHIRANI, R. (2007). On the “degrees of freedom” of the lasso. *Annals of Statistics*, **35** 2173–2192.